BMC Genomics

RESEARCH Open Access

Genome-wide identification and expression pattern analysis of *NAC* family in *Taxus yunnanensis* and the *TyuNAC30* role in paclitaxel production

Jiangtao Fan[1,3], Yong Wang[2,3*], Mengke Dou[1,3], Qiuhong Hu[1,3], Qing Li[1,3], Shengmei Gan[1,3], Mingwei Jing[1,3], Gang Wang[1,3*] and Xiong Huang[1,3*]

Abstract

Background The *NAC* transcription factor family represents a large group of plant-specific genes involved in various biological processes, including secondary metabolite biosynthesis, responses to biotic and abiotic stresses, and hormone signaling. *Taxus yunnanensis*, a well-known medicinal plant, is the natural source of the anticancer diterpene paclitaxel. Despite the biological importance of NAC transcription factors, no comprehensive genome-wide study of the NAC gene family has been conducted in *T. yunnanensis*.

Results In this study, 44 NAC genes were identified from the *T. yunnanensis* genome. Gene structure analysis revealed that the number of exons ranged from 1 to 7, with most genes containing 2 to 3 exons. Chromosomal mapping showed an uneven distribution of *TyuNACs* across the 11 chromosomes. Duplication type analysis indicated that dispersed duplication is the primary mechanism driving the expansion of the *TyuNACs*, accounting for the largest proportion (24 genes), followed by tandem (12 genes) and proximal duplications (8 genes); no whole-genome or segmental duplication events were detected. Cis-regulatory element analysis suggested that *TyuNACs* are involved in key biological processes such as development, light response, stress adaptation, and hormone signaling. Expression profiling revealed diverse tissue-specific expression patterns, with most *TyuNACs* highly expressed in bark. Moreover, qRT-PCR analysis demonstrated that several *TyuNACs* respond to methyl jasmonate (MeJA) treatment. Yeast one-hybrid and related assays revealed that *TyuNAC30* functions as a negative regulator of *TyuDBTNBT*, a key enzyme gene in the paclitaxel biosynthetic pathway.

Conclusion This study presents the comprehensive genome-wide characterization of the NAC transcription factor family in *T. yunnanensis*. The findings underscore the predominant role of dispersed duplication in the expansion of the *TyuNAC* family, with additional contributions from tandem and proximal duplications. Importantly, *TyuNAC30* was

*Correspondence:
Yong Wang
wangyong2015@sicau.edu.cn
Gang Wang
wanggang@sicau.edu.cn
Xiong Huang
huangxiongcaf@163.com

Full list of author information is available at the end of the article

identified as a negative regulator of *TyuDBTNBT*, suggesting a key role in the transcriptional regulation of paclitaxel biosynthesis. These findings offer valuable insights for further exploration of the functional roles of *NAC* genes, particularly their involvement in the regulatory mechanisms underlying paclitaxel biosynthesis.

Keyword Genome-wide identification, *Taxus yunnanensis*, *NAC* family genes, Paclitaxel biosynthesis, Expression pattern

Background

The genus *Taxus*, belonging to the Taxaceae family and commonly known as yews [1], consists of slow-growing, long-lived gymnospermous trees or shrubs [2]. These plants are considered relict species from the Tertiary period and exhibit a wide distribution across various countries [3], including regions in Asia, Europe, and North America. Presently, they are encountering endangerment [4]. In Nepal, *Taxus* is recognized as a crucial herbal remedy and has demonstrated a notable efficacy in treating conditions such as gastrointestinal disorders, coughs, and colds [5]. *T. yunnanensis* is predominantly found in Yunnan Province, China, and is a significant plant within the genus *Taxus*. It has been extensively researched due to its high-value secondary metabolite, paclitaxel, which is contained within its tissues [6, 7]. Since 1995, when Zhang et al. [8] first isolated and characterized the chemical constituents of *T. yunnanensis*, more than 100 paclitaxane diterpenes have been identified from various parts of the plant. Paclitaxel is a naturally occurring compound present in plants in minute quantities [9]. It is classified as a polyoxygenated cyclic diterpenoid and is widely utilized in clinical settings for treating diverse cancers such as ovarian, breast, lung, and cervical cancers [10–12]. The biosynthesis of paclitaxel is an extraordinarily intricate process that commences in vivo with the diterpene precursor geranylgeranyl diphosphate (GGPP) [13]. Subsequently, it undergoes a sequence of modifications catalyzed by cytochrome P450 hydroxylases (CYP450s), acyltransferases, and other enzymes, culminating in the production of the final product, paclitaxel [14–16]. However, due to the low natural concentration of paclitaxel in specific organs such as taxus bark [17], increasing its content has proven to be a significant challenge.

Transcription factors (TFs) are proteins that regulate gene expression by binding to specific cis-promoter regions of target genes, thereby either enhancing or inhibiting the transcription rate of those genes [18]. The NAC (NAM, ATAF1/2, and CUC2) family represents one of the largest plant-specific transcription factor families, named after its principal members: NAM (no apical meristem), ATAF1/2 (transcription activation factor), and CUC (cup-shaped cotyledon) [19]. NAC proteins consist of a highly conserved N-terminal domain (NAC domain) and a variable C-terminal domain [20]. The N-terminal domain, composed of 150 amino acids, is further subdivided into five distinct subdomains with specific functions: The A subdomain is associated with dimerization, while the B and E subdomains contribute to protein functional diversity. The C and D subdomains are involved in DNA binding interactions [21, 22]. The C-terminal region of NAC TFs is additionally involved in the regulation of transcriptional activation/inhibition regions (TAR or TRR), contributing to transcriptional regulation [23]. NAC transcription factors play a crucial role in regulating the expression of multiple target genes, involving their binding to specific DNA sequences (CATGTG motif) located within the promoter regions of these target genes [24].

NAC transcription factors (TFs) have been documented to control several developmental processes in numerous plant species. These activities include the formation of plant roots [25], the differentiation and division of cells [26], the development and aging of leaves [27], the maturation of fruits, and the germination of seeds [28]. Furthermore, NAC transcription factors (TFs) have a significant function in the cellular response to abiotic stressors, including salt [29], low and high temperature [30, 31], and drought [32]. Additionally, studies have demonstrated that NAC transcription factors play a role in controlling the production of secondary metabolites in plants [33]. These *NAC* TFs have been found to regulate the expression of genes involved in the secondary metabolite pathway, resulting in an enhanced production of valuable medicinal compounds [34, 35]. The emerging field of *NAC* transcription factors involves the coordinated regulation of secondary metabolite production, encompassing the analysis of net output, evocation of signals, and control over signaling pathways [36]. For example, overexpression of *AaNAC1* in *Artemisia annua* resulted in a substantial increase in sesquiterpene lactones content, including artemisinin and dihydroartemisinic acid [33], and *AaNAC2*, *AaNAC3*, and *AaNAC4* have been reported to bind to the promoter of the terpene synthase gene *AaTPS1*, thereby enhancing monoterpene production in *Actinidia chinensis* [37]. *SlNAC4* positively regulates carotenoid accumulation in *Solanum lycopersicum* [38]. In addition, *PgNAC72* in *Panax ginseng* was found to bind to the NAC-binding element within the *PgDDS* promoter, thereby activating its transcription and leading to a substantial increase in total saponin production [39]. Moreover, The production of caffeine in *Camellia sinensis* [35] and the production of

paeoniflorin in *Andrographis paniculata* are both regulated by NAC transcription factors [36]. Thus, NAC transcription factors play crucial roles in the regulation of plant secondary metabolite synthesis and have been reported in numerous plants [40], particularly in medicinal species. Nonetheless, little is known about the NAC transcription factor family in *T. yunnanensis*. MeJA is an important signaling mediator that regulates plant growth and development [41], and it has been shown to strongly promote the biosynthesis of taxoid compounds [42, 43]. However, MeJA induces paclitaxel biosynthesis in a concentration-dependent manner, exhibiting a saturation effect [44]. The response of paclitaxel biosynthesis to MeJA concentration increases linearly between 0 and 200 μM, but concentrations greater than 200 μM exhibit inhibitory effects [45]. Therefore, many studies use 100 μM as the optimal induction concentration and apply it in the transcriptional regulation studies of metabolites [39, 41].

Despite the resolution of the reference genome of *T. yunnanensis* [3], the investigation into *NAC* transcription factors in this species remains largely unexplored, with only a few studies to date identifying potential *NAC* transcription factors that could play a pivotal role in paclitaxel biosynthesis [46]. Therefore, further efforts are required to conduct comprehensive research on the *NAC* family. In this study we identified 44 *NAC* genes from the genomic data of *T. yunnanensis*. In addition to analyzing the gene structures, motifs, chromosomal locations, co-locations, subcellular localizations, and cis-acting elements, these genes were categorized based on their phylogenetic relationships with *Ginkgo biloba* NAC proteins. Additionally, the expression patterns and co-expression networks of the *TyuNAC30* and paclitaxel biosynthesis genes in various tissues were examined, and yeast one-hybrid crosses were used to confirm the regulatory effects of *NAC* on the paclitaxel biosynthesis genes. The findings of this work establish the groundwork for future enhancements of paclitaxel content via genetic modification and artificial regulation. They also offer significant insights into the molecular mechanism of transcriptional regulation of paclitaxel biosynthesis and optimization of the transcriptional regulatory network.

Materials and methods

Identification and classification of *NAC* genes in *T. yunnanensis*

The genome data of *T. yunnanensis* and *G. biloba* were retrieved from the 1 K Medicinal Plant Genome Database for further analysis (http://www.herbgenome.com/) and Ginkgo Genome Database (https://ginkgo.zju.edu.cn/). The NAC domain (PF02365), obtained from the Pfam protein family database, was employed in an HMM search against the protein database to identify all NAC-domain-containing proteins in *T. yunnanensis*. The NAC gene was searched using HMMR 3.0 with default settings and an E-value threshold of $1e^{-10}$ to identify relevant sequences [47]. To further investigate the structural features of the NAC genes identified in *T. yunnanensis* with NAC domains, we conducted additional analyses using SMART (http://smart.embl-heidelberg.de) and NCBI's conserved domain databases (CDD; https://www.ncbi.nlm.nih.gov/Structure/cdd/cdd.shtml). In addition, we evaluated various physicochemical properties, including subcellular localization, grand average of hydropathicity (GRAVY), isoelectric point (PI), and molecular weight (MW). A Perl script was employed to calculate the molecular weight and isoelectric points, while GRAVY values were computed using ExPASy (http://web.expasy.org/protparam/), and subcellular localization was predicted using WoLF PSORT (https://www.genscript.com/wolf-psort.html), CELLO (http://cello.life.nctu.edu.tw/) and Plant-mPLoc (http://www.csbio.sjtu.edu.cn/bioinf/plant-multi/).

Phylogenetic analysis and classification of *NAC* genes

A rooted neighbor-joining (NJ) phylogenetic tree of *T. yunnanensis*, *Arabidopsis* and *G. biloba* NAC proteins was generated using MEGA 7 software to investigate their evolutionary relationships and classify the NAC gene family [48]. Protein sequences for *Arabidopsis* and *G. biloba* NACs were obtained from the TAIR11 database (https://www.arabidopsis.org) and Ginkgo Genome Database (https://ginkgo.zju.edu.cn/). Sequence alignment was performed using ClustalW with the default parameters, and the phylogenetic tree was visualized and refined using Evolview2 [49].

Analysis of gene architecture and conserved motifs

To predict motifs, the TyuNAC protein sequence was input into the MEME online tool (http://meme-suite.org/) [47]. The pattern discovery was set to identify 10 motifs, with the minimum and maximum motif widths and repetition numbers configured accordingly. The NAC motif domain was visualized using TBtools [50]. Additionally, the online Gene Structure Display Server (GSDS) (http://gsds.cbi.pku.edu.cn/index.php) was employed to illustrate the gene structure and extract the locations of the NAC gene sequences from the genome annotation file.

Analysis of chromosomal locations, gene duplication and collinearity

A total of 44 NAC genes were mapped onto chromosomes, and their distribution was visualized using Map Chart software (v2.32) [51]. Gene duplication analysis was performed using MCScanX (https://github.com/wyp1125/MCScanX). Collinearity among all proteins in the *T. yunnanensis* genome was first identified, followed by

classification of gene duplication types with the built-in duplicate_gene_classifier module. Long terminal repeat (LTR) retrotransposons were detected using EDTA (v2.2.0), and NAC gene duplication types were subsequently extracted based on MCScanX results [52]. Nonsynonymous (Ka) and synonymous (Ks) substitution rates were calculated using KaKs-Calculator [53]. Additionally, MCScanX (v1.0.0) was used to analyze syntenic relationships between *T. yunnanensis NAC* genes and those from *A. thaliana*, *G. biloba*, *Phellodendron amurense*, *Catharanthus roseus* and *Salvia miltiorrhiza*.

Promoter cis-regulatory element analysis of *TyuNAC* genes

The 2000 bp upstream sequence of the *TyuNAC* gene was extracted from the genome file and submitted to the Plant-Care website (http://bioinformatics.psb.ugent.be/webtools/plantcare/html) for cis-acting element prediction . The findings from the Plant-Care analysis were summarized, and TBtools was used to visualize the results [50].

Expression pattern and functional annotation analyses of *TyuNAC* genes

To gain deeper insights into the expression patterns of the *TyuNAC* gene across various tissues and organs, transcriptomic data for five tissue types were retrieved from the NCBI database [3]. The tissues studied included bark, leaf, root, stem, and twig bark, with data sourced from the public transcriptome repository (BioProject: PRJNA661543). All datasets were generated from three independent biological replicates. The data were processed and visualized using TBtools software [50]. GO annotation of the *TyuNAC* gene set was carried out using GOATOOLS (https://github.com/tanghaibao/GOatools) based on GO terms derived from the Gene Ontology Consortium. Enrichment analysis was performed using Fisher's exact test, and Bonferroni correction was employed to adjust for multiple comparisons. GO terms with $P < 0.05$ were deemed significantly enriched, reflecting the overrepresentation of specific biological functions within the *TyuNAC* gene set [54].

Expression analysis using quantitative real-time polymerase chain reaction (qRT-PCR)

The experimental materials consisted of two-year-old *T. yunnanensis* seedlings, which were disease- and pest-free, with similar heights (50–60 cm) and growth conditions. Seedling-stage plants were selected for sampling due to their uniform developmental status, which helps minimize biological variation. Previous studies have also indicated that key genes involved in paclitaxel biosynthesis show higher expression during early developmental stages, suggesting that the seedling phase may reflect an active period of secondary metabolite accumulation [55]. The *T. yunnanensis* were planted in Dujiangyan city, Sichuan Province, China (31.01°N, 103.37°E). *T. yunnanensis* seedlings were treated with 100 μmol/L MeJA (Sigma, Santa Clara, CA, USA) each with three replicates (n = 3). Samples of leaves and bark were collected at 0 h, 3 h, 6 h, 9 h, 12 h, and 24 h post-treatment for gene expression analysis. The collected samples were immediately flash-frozen in liquid nitrogen and then stored in an ultra-low-temperature freezer (Thermo, Waltham, MA, USA) for further analysis [56]. All tissues were collected from three individual trees as biological replicates.

Total DNA and RNA was extracted from leaf sample using the CTAB method, and the cDNA was obtained using PrimeScript® II first Strand cDNA Synthesis Kit (TaKaRa, Japan). The qRT-PCR was referred to our previous experimental operation in a Bio-Rad CFX96™ system (Bio-Rad, America), and *TyuActin* was selected as internal control. The specific primers were designed by Primer Premier 5.0 with amplified PCR products from 80 to 300 bp. All qRT-PCR primers were evaluated for amplification efficiency using standard curve analysis with serially diluted cDNA. Only primers with efficiency values ranging from 90 to 110% and correlation coefficients (R^2) above 0.99 were considered acceptable for gene expression quantification (Tables S1-S2). The relative expression levels of the genes across different samples were calculated using the $2^{-\Delta\Delta Ct}$ method to compare the relative expression of each gene in 0 h of each treatment and control condition, and three biological replicates were conducted for each gene. Data alignment and analysis were conducted using Excel 2019, and graphical representations were generated with GraphPad Prism 5 [57].

Protein–protein interaction network analysis

The genomic protein sequences of *T. yunnanensis* were compared with those of *A. thaliana* using the online server OrthoVenn2 (https://orthovenn2.bioinfotoolkits.net/home) to map homologous gene relationships. The NAC protein interaction network of *T. yunnanensis* was analyzed using the online website String (https://string-db.org/). Protein interaction networks were visualized using Cytoscape software (version 3.9.0).

Content determination of paclitaxel and 10-Deacetylbaccatin III (10-DAB) under MeJA treatment

1.0 g of powdered dried *T. yunnanensis* branches and leaves was added to 15 mL of methanol and extracted using an ultrasonic device (KQ5200DE, Kunshan Ultrasound Instrument Company, Kunshan, China) for 1 h and three biological replicates were conducted for each sample. The extract was centrifuged at 5000 rpm for 5 min to obtain the supernatant. The supernatant was transferred to a 50 mL volumetric flask and filtered through a 0.45 μm microfiltration membrane. Paclitaxel and 10-DAB were analyzed using a Shimadzu

LC20AB high-performance liquid chromatography (HPLC) system. The paclitaxel and 10-DAB determination were separated on a Phenomenex Luna C18 column (4.6 mm × 250 mm, 5 μm) with mobile phases consisting of acetonitrile and water in ratios of 45:55 (v/v) and 29:71 (v/v), respectively. Detection was performed at 227 nm with a flow rate of 1 mL/min, an injection volume of 10 μL, and a column temperature of 30 °C. Quantitative analysis was performed using standard solutions of paclitaxel and 10-DAB to establish a calibration curve (Tables S3), representative chromatogram is shown in Fig S1. The standards, 10-DAB (≥ 98%, CAS: 32,981–86-5) and paclitaxel (≥ 99.9%, CAS: 33,069–62-4), were procured from Beijing Solarbio Science & Technology Co., Ltd. (Beijing, China).

Subcellular location analyses of AspbHLH

The CDS region of *TyuNAC30* (excluding its stop codon) was inserted into the *pCAMBIA1300-35S: GFP* vector. Snap Gene 6.0.2 software was used to design the amplification primers for the constructed plasmid, which was introduced into *Agrobacterium tumefaciens* GV3101 using the conventional freeze–thaw method, and then subsequently infiltrated into 5-week-old tobacco leaves (*Nicotiana benthamiana*) at 5 weeks of age [58]. The GFP signal was then detected using a Leica confocal microscope 3 days after infestation.

Yeast one-hybrid assays

The CDS of *TyuNAC30* was inserted into the pGADT7 vector to generate the recombined constructs *AD- TyuNAC30*. Referring to previous studies, promoter fragments of the DBTNBT genes were cloned from *T. yunnanensis* and inserted into the pAbAi vector [59]. The co-transformed Y1H Gold yeast strains were plated on SD/-Leu plates with or without AbA.

Luciferase complementation imaging assay

The LUC assay was employed to verify the interaction between TyuNAC30 and TyuDBTNBT. *TyuNAC30* and the promoter sequences of *TyuDBTNBT* were cloned into the *pGreen II 62-sk* and *pGreen II 0800-LUC* vectors, respectively. These vectors were then transformed into Escherichia coli, and bacterial cultures containing the correctly identified plasmids were obtained. Subsequently, the extracted plasmids, along with empty *pGreen II 0800-LUC* and *pGreen II 62-sk* vectors as controls, were transformed into *Agrobacterium* strain GV3101 containing pSoup plasmid. Then, the four vectors were separately mixed in pairs and injected into tobacco leaves, following established protocols [58]. The injected leaves were first kept in darkness for 24 h and then transferred to a standard incubator for 12 to 24 h for further experimentation. LUC fluorescence was subsequently observed using a multicolor fluorescence imaging system. Three biological replicates for each treatment were performed.

Statistical analyses

Data were processed using Microsoft Excel 2016. All values are presented as the mean ± standard deviation (SD) from at least three biological replicates. Statistical analyses were performed using GraphPad Prism 8.0. The one-way ANOVA test and Tukey's test were used to assess differences, with $p < 0.05$ considered statistically significant.

Results

Identification and classification of NAC genes in *T. yunnanensis*

In the genome of *T. yunnanensis*, a total of 44 *TyuNAC* genes were identified, each designated as *TyuNAC1* to *TyuNAC44* based on its chromosomal position. The fundamental physicochemical properties of TyuNAC proteins are detailed in Table S4, encompassing characteristics such as molecular weight (MW), isoelectric point (pI), hydrophobicity, and subcellular localization predictions. The molecular weights of TyuNAC proteins in this study ranged from 5.87 to 63.85 kDa, with corresponding pI values spanning 6.70 to 111.62. Hydrophobicity predictions indicated GRAVY scores ranging from −0.904 to 0.294, where all 44 proteins exhibited negative values, indicative of their hydrophilic nature. Regarding subcellular localization, predictions indicated that 41 of the 44 TyuNAC proteins were in the nucleus, while 2 were found in the cytoplasmic nucleus, and 1 was located extracellularly.

Phylogenetic analysis of TyuNAC proteins

To investigate the evolutionary relationships of TyuNAC proteins, a phylogenetic tree was constructed using amino acid sequences from 44 TyuNACs, 144 AtNACs (from *A. thaliana*), and 50 GbNACs (from *G. biloba*). Based on homology with *G. biloba* NAC proteins, the TyuNAC proteins clustered into nine branches, designated as Group I to Group IX subgroups (Fig. 1). The largest groups, Groups VII, each include 12 TyuNAC members, while the smallest, Groups II and IV, comprise only 2 members each. Furthermore, similar functional GbNAC and AtNAC proteins tend to cluster within the same subgroup. For instance, VND1 (AtNAC037), VND2 (AtNAC076), VND3 (AtNAC105), VND4 (AtNAC007), VND5 (AtNAC026), VND6 (AtNAC101), and VND7 (AtNAC030), associated with secondary wall synthesis, are mainly grouped in Group VI (Table S5). Consequently, it is hypothesized that TyuNAC proteins within corresponding subgroups may share similar functions.

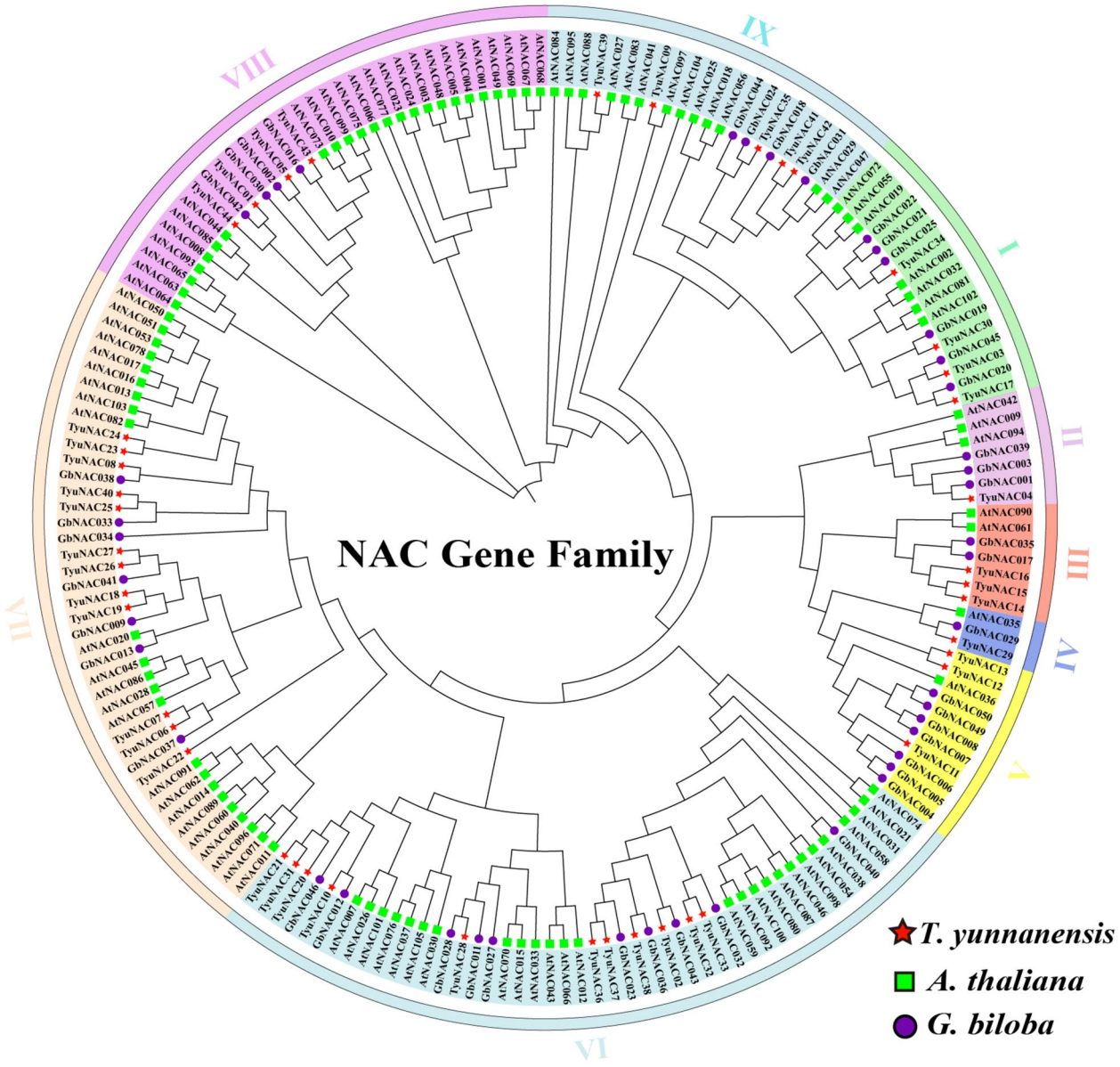

Fig. 1 Phylogenetic tree of NAC proteins between *T. yunnanensis*, *A. thaliana* and *G. biloba*. They are divided into 9 subgroups according to the subgroups of *G. biloba* and represented by different colors. The red star, green square and purple circle represent *T. yunnanensis* (prefix as Tyu), *A. thaliana* (prefix as At), and *G. biloba* (prefix as Gb), respectively

Gene structure, conserved motifs, and domain analysis of *TyuNAC* genes

To gain deeper insights into the structural diversity and similarity among *TyuNAC* genes, we analyzed conserved motifs and intron/exon distributions according to their phylogenetic relationships (Fig. 2A-D). Using the MEME program, we predicted a total of 10 conserved motifs, designated as motif 1 through motif 10 (Fig. 2E, Table S6). All *TyuNAC* genes exhibit five NAC sub-structural domains (A-D), as illustrated in Fig. S2. Consistent with structural domain analysis, clustered *TyuNAC* members share common motif compositions, suggesting potential functional similarities. Specifically, the N terminus of most *TyuNAC* genes contains three conserved motifs (motif 2, motif 4, motif 5). Analysis of intron/exon structures in *TyuNAC* coding sequences revealed variability, with some genes featuring multiple untranslated region (UTR) regions while others lack such structures. This diversity likely reflects evolutionary distinctions among homologous *TyuNAC* genes. Intriguingly, *TyuNAC* genes within the same phylogenetic group exhibit highly similar intron/exon structures, primarily differing in the lengths of exonic and intronic regions.

Fig. 2 The phylogenetic and gene structure analyses of *TyuNAC* genes. **A** The phylogenetic classification of *TyuNACs*. **B** Conserved motif analysis of *TyuNACs*. A total of 10 predicted motifs are represented by different colored boxes. **C** Domain pattern analysis of *TyuNACs*. **D** Gene structure analysis of *TyuNACs*. The yellow boxes and green boxes represent UTR and CDS and the black dashes are introns. **E** The sequence logos of ten motifs. The height of each letter indicates the degree of conservation. Numbers on the x-axis represent residue positions, and the y-axis represents the content measured in bits

Analysis of promoter cis-regulatory element of *TyuNAC* genes

In this study, we identified 44 cis-regulatory elements (CREs) in the promoter regions of the *TyuNAC* genes. These CREs were classified into three main categories based on their functional roles: hormone-responsive elements, plant growth and development-associated elements, and biotic and abiotic stress-responsive elements (Fig. 3). Detailed information on the *T. yunnanensis* cis-regulatory elements is provided in Table S7. The analysis revealed that abiotic stress-responsive elements were the most abundant among the identified CREs, followed by

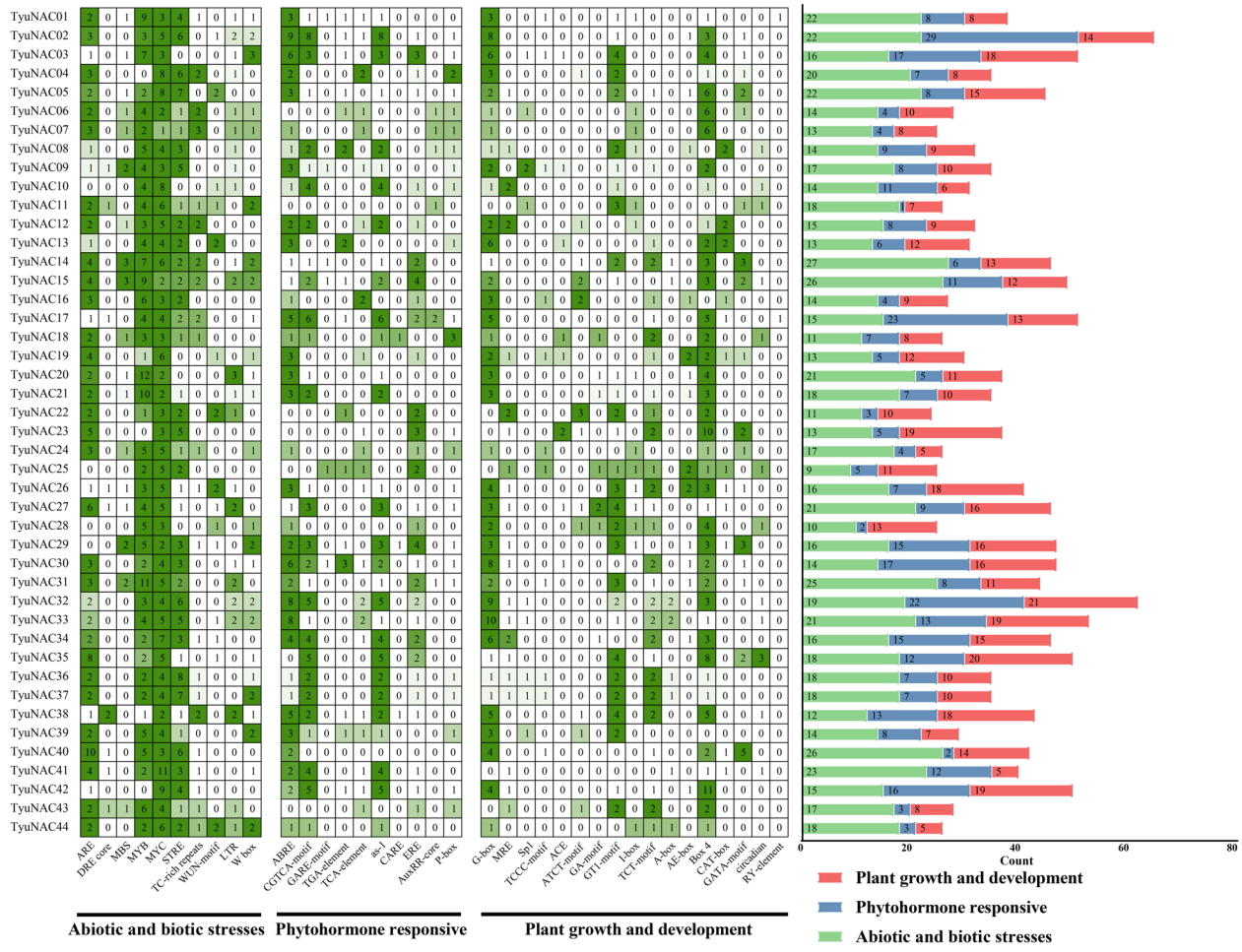

Fig. 3 The cis-regulatory elements analysis of *TyuNACs* promoter regions. **A** Statistics for cis-acting elements in the promoter regions of *TyuNAC* genes. The numbers of specific cis-elements are indicated by numbers and a green color gradient. **B** Color-coded histograms indicate the numbers of cis-elements in each category

hormone-responsive elements and those associated with plant growth and development (Fig. 3). This distribution suggests a strong correlation between *TyuNAC* gene expression and environmental stress responses. Notably, the number of abscisic acid (ABA)-responsive elements (ABREs) was significantly higher than that of other phytohormone-related elements, indicating a potentially crucial role for ABA in the regulation of *TyuNAC* gene expression in *T. yunnanensis*.

Gene duplication, chromosomal distribution, and synteny analysis of *TyuNAC* gene

Genomic locations of *TyuNACs* were obtained from annotation files, revealing their non-random distribution across 11 chromosomes; chromosome 12 lacked *TyuNACs*. Chromosome 5 had the most *TyuNACs* (7, 15.91%), followed by chromosome 4 (6 genes, 13.64%) (Fig. 4A). Analysis of gene duplication types revealed that a total of 24 *TyuNACs* originated from dispersed duplications, 12 from tandem duplications, and 8 from proximal duplications, whereas no whole-genome duplication (WGD) or segmental duplication events were detected (Fig. 4B, Table S8). Ka/Ks ratios indicated these duplicates evolved under negative purifying selection (Table S9). Synteny analysis with *A. thaliana* revealed no homologous *NAC* genes. To explore syntenic relationships in more closely related species, additional comparisons were conducted. In *G. biloba*, 24 syntenic NAC genes were identified, indicating a relatively high level of collinearity with *T. yunnanensis*. In addition, syntenic NAC genes were detected in three representative medicinal plants: three in *P. amurense*, one in *S. miltiorrhiza*, and one in *C. roseus*. These results suggest that NAC genes in *T. yunnanensis* exhibit greater syntenic conservation with gymnosperms and selected medicinal plants than with *A. thaliana* (Fig. 4C-G).

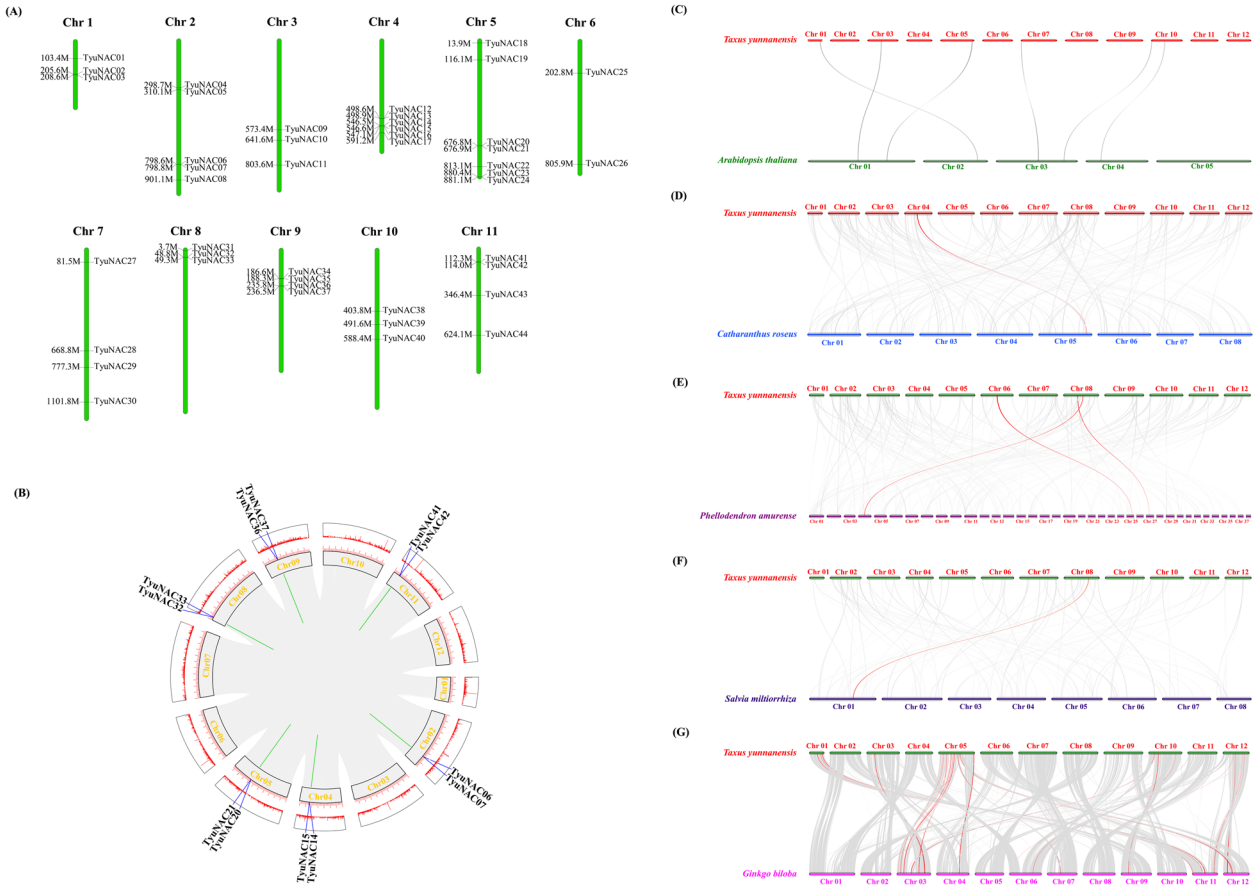

Fig. 4 Chromosomal locations, tandem duplications of *TyuNAC* genes, and synteny analysis of *TyuNAC* genes with *A. thaliana*, *C. roseus*, *P. amurense*, *S. miltiorrhiza*, and *G. biloba*, respectively. **A** Chromosomal locations of the *TyuNAC* genes. The number represents the position of the gene on the chromosome (M), (**B**) Synteny analysis of *TyuNAC* genes. Green lines connect fragments of repeated gene pairs, the grey lines are co-linear blocks in the species. **C**-**G** Synteny analysis of *TyuNAC* genes with five species, respectively. Red lines connect fragments of repeated gene pairs, the gray lines were the co-linear blocks among the species

Expression pattern, GO enrichment and protein–protein interaction network analysis of *TyuNACs*

To further elucidate the expression patterns of NAC family genes and their involvement in the growth, development, and synthesis of secondary metabolites in *T. yunnanensis*, the expression of *TyuNACs* was extracted from transcriptome data derived from five tissues (Table S10). Some genes showed patterns of tissue-specific expression, as shown in Fig. 5A-B. Some genes, like *TyuNAC13*, *TyuNAC16*, and *TyuNAC31*, only showed high expression in the Bark tissue, according to analysis of differentially expressed genes. This suggests that these genes may play important roles in the development of the Bark. *TyuNAC08*, *TyuNAC35*, *TyuNAC29*, and *TyuNAC41* genes were highly expressed only in leaves, suggesting that they may be associated with leaf growth and development. Notably, several *TyuNACs* showed root-specific high expression. For instance, TyuNAC10 exhibited a 34-fold higher expression in roots compared to bark ($\log_2$FC = 5.09), suggesting a potential role in root development. Although most of the *TyuNACs* showed differences in different tissues, indicating the diversity of their functions in different tissues, these inferences need to be further verified. GO enrichment analysis revealed that five *TyuNAC* genes were associated with the regulation of the flavonoid biosynthetic process (GO:0009962) (Fig. 5C), indicating a potential involvement of *TyuNACs* in secondary metabolite biosynthesis (Table S11). Furthermore, promoter analysis showed that several key enzyme genes involved in flavonoid and paclitaxel biosynthesis contain putative NAC binding motifs (Fig. S3), suggesting that *TyuNACs* may directly regulate these pathways at the transcriptional level. After analyzing the expression of enzyme genes involved in the paclitaxel biosynthetic pathway, it was noted that these enzyme genes showed distinct tissue-specific expression patterns. Notably, most enzyme genes exhibited high expression levels in the bark (Fig. 5B), resembling the expression patterns observed in specific *TyuNACs*. In summary, *TyuNACs* may play a potential role in the biosynthesis of the diterpene alkaloid paclitaxel. Additionally, we predicted interactions among *TyuNACs* and identified that

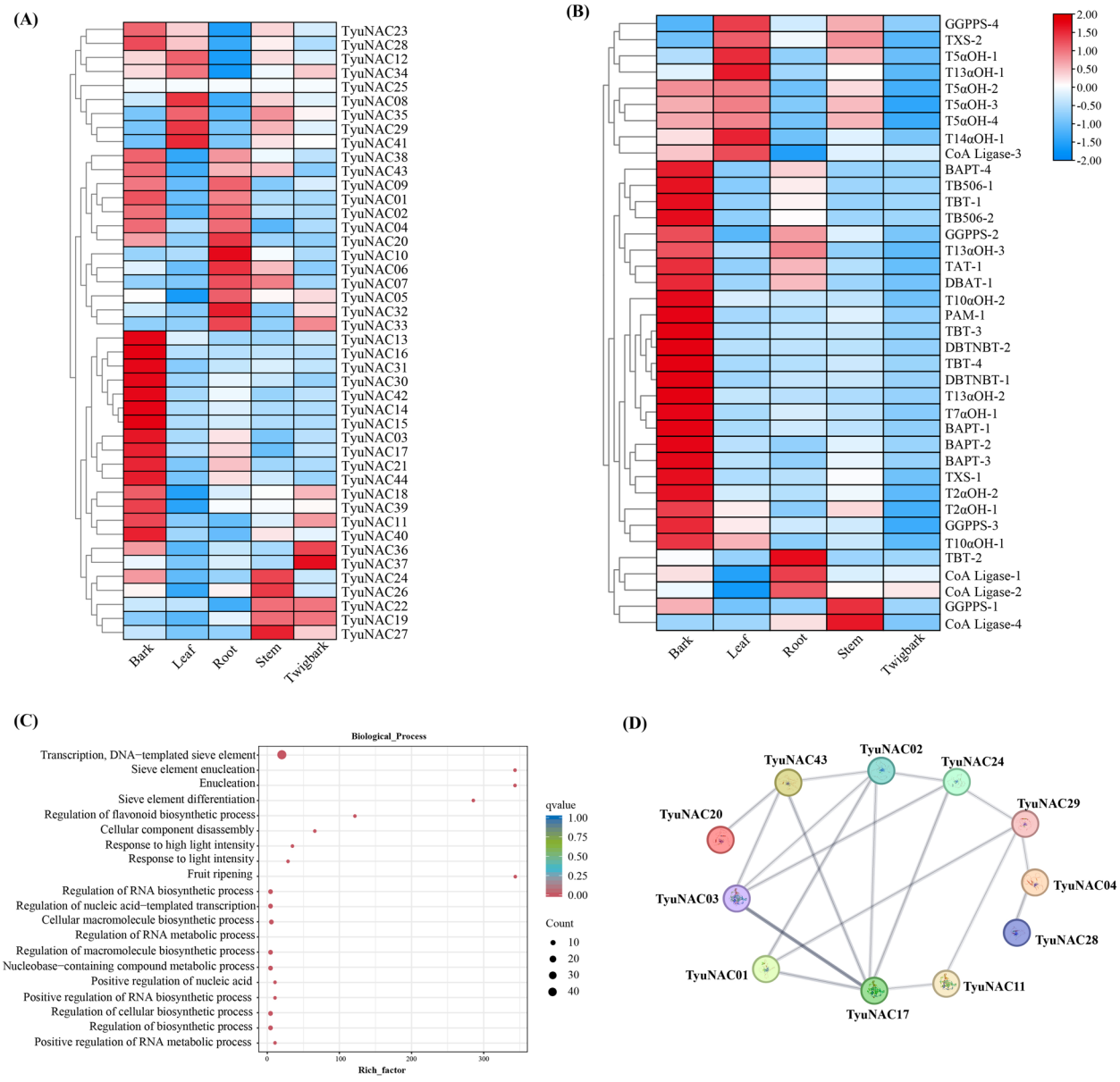

Fig. 5 Expression patterns of *TyuNAC* genes in different tissues based on transcriptome datasets. **A**-**B** Expression heatmap of *TyuNACs* in root, stem, leaf, twigbark, and bark. The color bars were the relative expression levels after column scale, and the data in each heatmap were the original FPKM values of the samples. **C** GO analysis result of all identified *TyuNACs*. The red represents significantly enriched; the size of the pot represents enriched gene numbers. **D** Protein–protein interaction network analysis of *TyuNACs*. Circles represent proteins, different colors represent different proteins, and inside the circle is the three-dimensional structure of the protein. Straight lines indicate the interactions between proteins. The thicker the line, the stronger the interaction

11 *TyuNACs* interacted with each other (Fig. 5D), with the most robust interactions observed between *TyuNAC03* and *TyuNAC17*.

MeJA-induced expression changes of *TyuNACs* and paclitaxel biosynthetic genes

To further investigate the impact of MeJA on the expression of *TyuNAC* gene, 18 *TyuNAC* genes were randomly selected to assess changes in their expression levels in leaves and bark at various time points following MeJA treatment (Fig. 6). The results observed that the expression of *TyuNACs* was obviously influenced by MeJA treatment. Specifically, *TyuNAC03*, *TyuNAC13*, and *TyuNAC44* genes exhibited a pattern of initial increase followed by a decrease in expression levels as the duration of treatment extended in leaf tissues (Fig. 6A, E, R). Similarly, *TyuNAC08*, *TyuNAC35*, and *TyuNAC39* displayed a similar trend in bark tissues (Fig. 6B, N, P). Notably, under MeJA treatment, the expression of the *TyuNAC17* exhibited significant changes in both leaf and bark tissues. In leaf tissue, 4 genes reached peak expression at 3 h post-treatment, whereas in bark tissue,

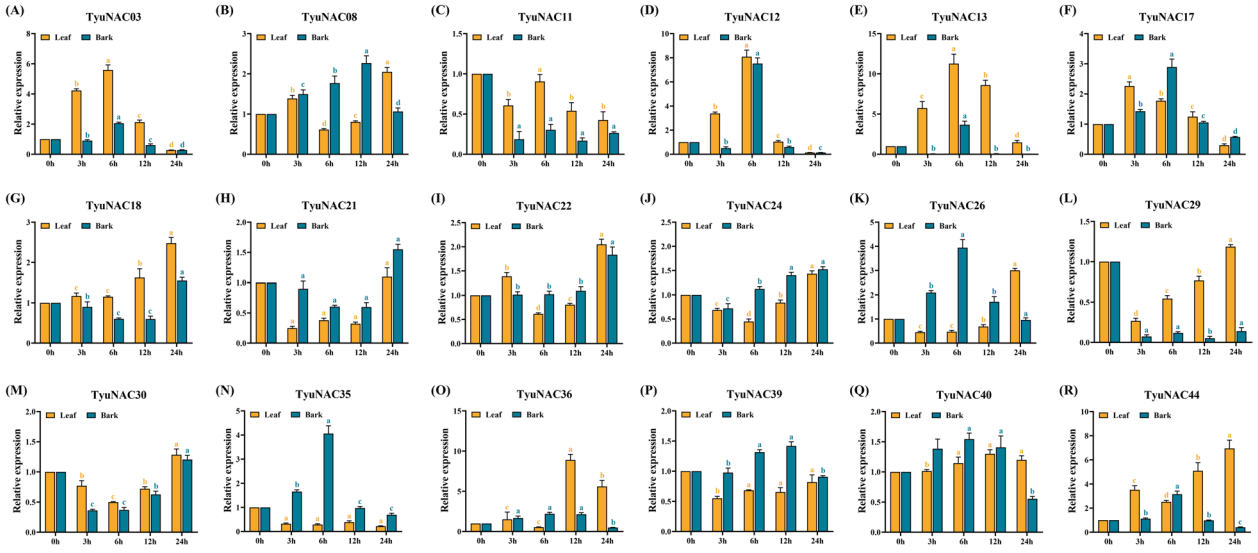

Fig. 6 Gene expression analysis of 18 *TyuNAC* genes under MeJA treatment using qRT-PCR. The 0 h was selected as the control sample to estimate the relative expression under MeJA treatment. Different letters in orange and blue indicate statistically significant differences among differentiated tissues for leaf and bark, respectively ($P < 0.05$), as determined by one-way ANOVA test

maximum expression occurred at 6 h post-treatment (Fig. 6A, E, M, R). This observation indicates that the expression pattern of *TyuNAC17* gene responds to MeJA treatment in a time-specific manner. Additionally, it was observed that MeJA treatment inhibited the expression of certain *TyuNACs*. For instance, *TyuNAC24* and *TyuNAC29* showed an initial decrease in expression immediately after treatment, followed by a gradual return to their original levels over time (Fig. 6J, L).

Additionally, the expression of paclitaxel synthase genes was significantly affected by MeJA treatment (Fig. S4A-F). In leaf tissue, all six genes were upregulated to varying degrees following MeJA treatment. For example, *TyuTAT* showed a rapid induction at 3 h (2.56-folds, $\log_2$FC = 1.36), while *TyuDBTNBT* expression peaked at 12 h (2.39-folds, $\log_2$FC = 1.26) and remained high at 24 h (2.22-folds) (Fig. S4C-D). *TyuTBT* also exhibited a progressive increase, reaching a maximum 2.05-folds at 24 h ($\log_2$FC = 1.03). Moderate increases were also observed for *TyuTS*, *TyuDBAT*, and *TyuBAPT*, with fold changes ranging from 1.4 to 2.4 across different time points. In bark tissue, the MeJA response was even more pronounced. *TyuTBT* expression rose dramatically to 5.27-fold at 3 h ($\log_2$FC = 2.40), maintaining elevated levels at 6 h (4.59-folds) and 12 h (3.70-folds). *TyuDBTNBT* increased significantly to 4.06-fold at 6 h ($\log_2$FC = 2.02) and remained elevated through 12 h and 24 h. *TyuTAT* expression also peaked at 6 h with a 2.99-fold increase, while *TyuTS*, *TyuDBAT*, and *TyuBAPT* showed upregulation between 1.5- to 2.4-folds at various time points.

Dynamic changes in paclitaxel and 10-DAB levels in response to MeJA treatment

To further investigate the effects of MeJA on the content of paclitaxel and 10-DAB compounds in the leaves and branches of *T. yunnanensis*, we examined the changes in the levels of paclitaxel and 10-DAB following MeJA treatment. The results indicated a significant increase in paclitaxel content in the leaves and branches after treatment (Fig. S4J), with levels beginning to rise at 3 h, peaking at 6 h, and then decreasing, reaching the baseline level by 24 h. In contrast, the 10-DAB content peaked at 3 h (Fig. S4H), gradually declined thereafter, but did not return to the initial level by 24 h.

Subcellular localization analysis of *TyuNAC* and functional analysis in paclitaxel biosynthesis

Transcriptome DEGs anaiysis have revealed that some *TyuNAC* exhibits specific high expression in the bark (Table S12), and shares a similar expression pattern with key enzyme genes involved in paclitaxel biosynthesis. Therefore, we hypothesize that *TyuNAC* may potentially play a role in paclitaxel biosynthesis. Subcellular localization analysis showed that TyuNAC30 was localized in the nucleus (Fig. 7A). To further explore the role of TyuNAC30 in the transcriptional regulation of paclitaxel biosynthesis, this study analyzed the cis-acting elements in the promoter sequences of key enzyme gene, *TyuDBTNBT*, and identified multiple NAC transcription factor-binding elements, including ABRE (Fig. 7B). Yeast one-hybrid results showed that yeast cells co-transformed with *AD-TyuNAC30* and *pAbAi-proTyuDBTNBT* grew colonies on triple-deficient plates, respectively, indicating that *TyuNAC30* directly binds to the promoter

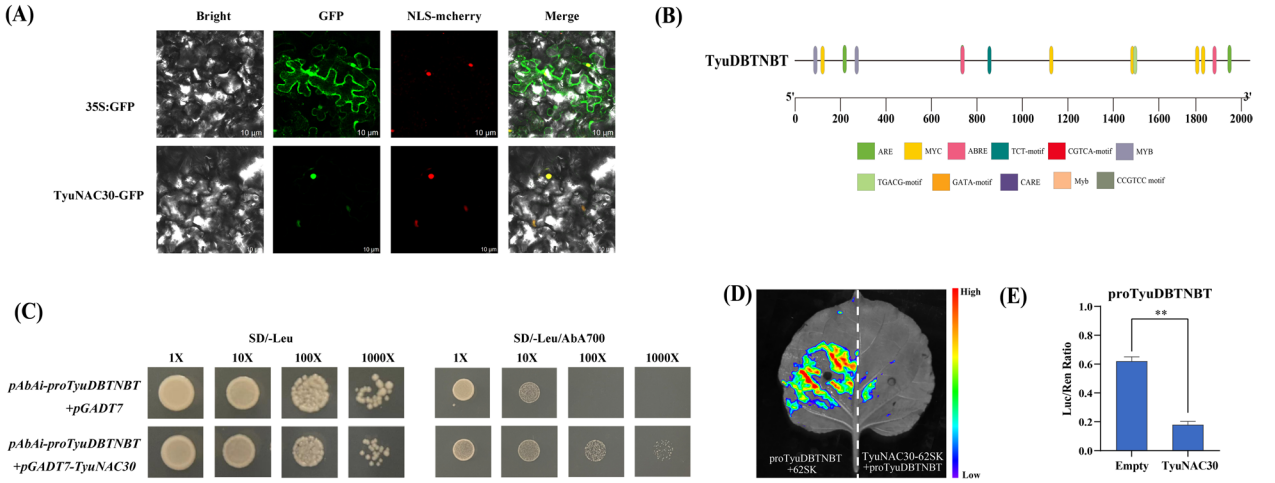

Fig. 7 *TyuNAC30* directly binds to *TyuDBTNBT* promoter to inhibit its expression. **A** Subcellular localization of TyuNAC30 protein in *N. benthamiana* leaves. **B** The cis-acting element analysis of *TyuDBTNBT* promoter. **C** Yeast one-hybrid (Y1H) assay showed that *TyuNAC30* directly binds to the promoter of *TyuDBTNBT*. **D**-**E** Luciferase (Luc) assays showed that *TyuNAC30* inhibits the transcription of *TyuDBTNBT*. (** indicates $P < 0.01$, one-way ANOVA test; error bar: SD)

of *TyuDBTNBT* (Fig. 7C). The Luc assay demonstrated that co-injection of *TyuNAC30 −62SK* with *proTyuDBTNBT* reduced the intensity of the Luc fluorescence signal compared to injection of *proTyuDBTNBT* alone (Fig. 7D). The Luc/Ren ratio was significantly lower than that of the control, indicating that *TyuNAC30* suppressed the promoter activity of *TyuDBTNBT* (Fig. 7E).

Discussion

Since the discovery of paclitaxel in the Pacific yew tree in 1971, the biosynthetic pathway has been extensively studied [60, 61]. During this time, several key genes encoding enzymes involved in paclitaxel biosynthesis have been identified and characterized [13, 62]. These findings have enhanced our understanding of the enzymatic processes underlying paclitaxel production. Recent genome sequencing of various Taxus species has significantly advanced our knowledge of paclitaxel biosynthesis [3, 63, 64]. These genomic data provide important insights into the transcriptional regulation of paclitaxel biosynthesis [65, 66]. Transcription factors are key regulators that activate biosynthetic genes at the transcriptional level [56]. and the MYB, bHLH, AP2/ERF, WRKY, and NAC families have been shown to play significant roles in paclitaxel regulation [46, 67, 68]. The involvement of NAC family members in plant growth and development under abiotic stress conditions, as well as their contributions to enhancing crop resistance, has been well-documented [19, 69]. However, their specific roles in the regulation of secondary metabolite synthesis remain to be more thoroughly investigated. This study systematically investigated the potential molecular functions of NAC genes in the transcriptional regulation of paclitaxel biosynthesis. In this study, we systematically identified the members of the *NAC* gene family in *T. yunnanensis* and performed extensive bioinformatics analyses to investigate their phylogenetic relationships, gene structures, motif compositions, chromosomal locations, tandem repeat sequences, and homologous genes. Furthermore, we explored the promoter cis-regulatory elements, tissue-specific expression profiles, and the regulatory functions of *NAC* genes in modulating the expression of key enzymes involved in paclitaxel biosynthesis. These findings provide valuable insights into the *NAC* gene family and lay the groundwork for future investigations into the functional roles of *NAC* genes in the biosynthesis of secondary metabolites (Fig. S5).

This study identified a total of 44 NAC gene family members, which is notably fewer than the 117 NAC genes found in *A. thaliana*, but comparable to the 46 NAC genes present in *Amborella. trichopoda*. Differences in the number of NAC gene family members among species may be attributable to various evolutionary events, such as gene rearrangements, amplifications, and contractions of gene families [70]. Using three widely recognized prediction tools we identified three *TyuNACs* predicted to localize outside the nucleus. Although experimental validation is still lacking, the consistent results across multiple tools provide useful references and suggest potential noncanonical functions worthy of further investigation. The structural analysis of the *TyuNACs* indicates that genes within different subgroups exhibit distinct structures and conserved motifs. In contrast, genes within the same subgroup share similar motif compositions and structural features [71]. This suggests that members of the same subgroup likely perform similar functions [72]. These results align with those observed in *A. thaliana*, *Oryza sativa*, and *Vitis viniferae* [73, 74], indicating that NAC proteins with comparable structures and motifs across these species are likely functionally orthologous.

TyuNACs family has many cis-acting elements associated with light responses, hormone responses, and biotic and abiotic stress responses. This is consistent with the discovery of other plant NAC gene families [75, 76]. In addition, it was found that many of the *TyuNACs* family members have multiple CGTCA motifs that function primarily as MeJA response elements, suggesting that NAC expression may be regulated by MeJA [77]. The evolution of gene duplication and genome size is closely related to the origin of new genes, species divergence, and gene mutation resistance [78–80]. Gene duplication events, particularly dispersed, tandem, and proximal duplications, contribute to the expansion and functional diversification of *TyuNACs*. The Ka/Ks ratio can indicate whether a gene is undergoing neutral, purifying, or accelerated evolution under positive selection [81]. In this study, the Ka/Ks ratio for all tandemly duplicated genes was less than 1, suggesting that *TyuNACs* primarily evolved under purifying selection. Comparative genomic analysis revealed marked differences in the size of the NAC gene family across species. Notably, *P. amurense* exhibited a substantial expansion (Table S13), suggesting possible lineage-specific gene duplications associated with the regulation of alkaloid and flavonoid biosynthesis [82]. Compared to gymnosperms such as *G. biloba*, angiosperm medicinal plants generally possess larger NAC families, which may reflect the increased complexity of their secondary metabolic pathways. *T. yunnanensis*, a gymnosperm, contains relatively fewer NAC genes, indicating a more conserved NAC repertoire with potentially specialized functions [83]. These findings support the hypothesis that NAC gene expansion and diversification may be evolutionarily linked to the regulation of specialized metabolism in medicinal plants.

Typically, analyzing gene expression patterns can reveal the potential functions of genes [72]. The results revealed that some *TyuNACs* exhibit tissue-specific expression patterns. For instance, *TyuNAC05* and *TyuNAC10* are highly expressed in roots, suggesting that these genes may be related to root development and stress resistance [84]. Furthermore, some *TyuNACs* genes, such as *TyuNAC13* and *TyuNAC16*, are specifically expressed only in the bark, which is also the primary site of paclitaxel production and accumulation in Taxus species [85]. Although the transcriptome data were derived from various tissues (e.g., root, stem, leaf, bark) and the qRT-PCR focused on MeJA-treated branches and leaves, both datasets showed complementary expression patterns. Several TyuNAC genes exhibited high tissue-specific expression and were significantly induced by MeJA, suggesting their potential roles in paclitaxel biosynthesis or other secondary metabolic pathways. Previous studies have indeed confirmed that NAC TF can regulate the expression of genes involved in paclitaxel biosynthesis [46]. MeJA is commonly used as an inducer of secondary metabolites. Previous studies have reported that MeJA treatment increases the accumulation of alkaloids and phenolics in plants and, in the case of *T. yunnanensis*, is also crucial for regulating paclitaxel levels [86, 87]. In our study, the paclitaxel content reached a maximum at 6 h following MeJA treatment but declined sharply to baseline levels by 24 h. This transient accumulation pattern has also been reported in other Taxus, such as *Taxus media* and *Cephalotaxus hainanensis*, where MeJA induces a rapid yet short-lived increase in paclitaxel levels [88, 89]. This dynamic likely reflects the kinetics of jasmonate signaling, which typically triggers immediate early gene activation followed by rapid attenuation. These findings suggest that while MeJA acts as an effective elicitor, its regulatory effects on paclitaxel biosynthesis are time-sensitive and may be subject to tight endogenous control. After MeJA treatment, some of *TyuNACs* was significantly induced or inhibited in bark and leaves, in addition, some of *TyuNACs* was also consistent with the trend of the expression of paclitaxel synthase genes, from which we hypothesized that there might be a potential regulatory role between *TyuNACs* and paclitaxel synthase genes. Therefore, the study also found that *TyuNAC30*, a transcription factor specifically expressed in the bark, exhibits expression changes after MeJA treatment that are inversely correlated with the expression of key paclitaxel biosynthesis enzymes (*TyuDBTNBT*) as well as the contents of paclitaxel and 10-DAB. Based on this observation, we hypothesize that *TyuNAC30* may be involved in the regulation of paclitaxel biosynthesis. Therefore, this study selected *TyuNAC30* for further validation. The results revealed that TyuNAC30 can bind to the promoters of key paclitaxel biosynthesis genes (*TyuDBTNBT*) and negatively regulate their expression (Fig. S4). Further analysis identified multiple NAC transcription factor binding sites (ABRA) within the promoter regions of these enzyme genes. Studies have shown that the NAC gene family interacts specifically with ABRE cis-regulatory elements [90]. Thus, we speculate that *TyuNAC* may bind to the ABRA element on the enzyme gene promoter to affect its expression. This is similar to the research results of *T. mairei*, where *DBTNBT* and *DBAT* have been identified as potential targets of *NAC2* [85]. Although this study demonstrated that *TyuNAC30* negatively regulates *TyuDBTNBT* expression, the functional relationship between TyuNAC30 and paclitaxel biosynthesis remains to be further validated through stable transgenic or gene silencing approaches to clarify its precise role in the regulation of paclitaxel synthesis. Functional characterization of *TyuNAC30* will be addressed in future studies.

TmNAC2 is also specifically expressed in the phloem [85], showing a similar expression pattern to *TyuNAC30*. Additionally, in *Taxus mairei*, *DBTNBT* and *DBAT*

have been identified as target genes of *TmNAC2*, and *TmNAC2* has been shown to repress the activity of the *DBTNBT* and *DBAT* promoters. This finding is consistent with the present study, which identified *TyuNAC30* as a negative regulator of *DBTNBT*. It has been reported that MeJA can induce the expression of NAC transcription factors [39]; however, the expression of *TyuNAC30* was suppressed, suggesting that MeJA may act as an inhibitor of *TyuNAC30*. These results collectively demonstrate that NAC transcription factors play roles beyond plant stress tolerance [72]. GO enrichment analysis revealed that NAC transcription factors are involved in the regulation of secondary metabolite biosynthesis, aligning with findings from other studies [70, 91–93]. Nevertheless, the exact mechanism of NAC regulation of paclitaxel biosynthesis remains to be further investigated.

Conclusions

In this study, we performed a comprehensive analysis of the *TyuNAC* transcription factor family in the *T. yunnanensis* genome. A total of 44 *TyuNAC* genes were identified, distributed across 11 chromosomes, and categorized into nine subfamilies. We also investigated their gene structures, conserved motifs, cis-regulatory elements, tissue-specific expression patterns, and expression changes under MeJA treatment. Tandem repeats were found to play a significant role in the expansion of the *TyuNAC* family. Some *TyuNAC* genes exhibited tissue-specific expression and were linked to plant secondary metabolite synthesis. Furthermore, TyuNAC30 was shown to negatively regulate the expression of TyuDBTNBT through binding to their promoters, as confirmed by yeast one-hybrid experiments and other experiments. Although *TyuNAC* influences the expression of paclitaxel biosynthesis genes, further research is needed to clarify its specific role in the paclitaxel biosynthetic pathway. Future studies should explore the interactions between *TyuNAC* and other key transcription factors, as well as their dynamic regulation under different growth stages and environmental conditions.

Supplementary Information

The online version contains supplementary material available at https://doi.org/10.1186/s12864-025-11916-z.

Supplementary Material 1: Table 1. Nucleotide sequences of primers used for gene cloning and vector construction. Table 2. Nucleotide sequences of primers used for qRT-PCR. Table 3. Regression equation of calibration curve for each ingredient. Table 4. Detailed information of ***TyuNAC*** genes. Table 5. The accession numbers of ***NAC*** genes in ***A. thaliana***. Table 6. The amino acid sequence of each conserved motif from each protein. Table 7. Cis-element analyses in promoter regions of 44 ***TyuNACs***. Table 8. Gene duplication type analyses of 44 ***TyuNACs***. Table 9. Ka, Ks and Ka/Ks of replication pairs of ***TyuNAC*** genes. Table 10. Expression of the ***TyuNAC*** genes in different tissues. Table 11. ***TyuNAC*** genes GO enrich biological process. Table 12. Differential expression analysis of ***TyuNACs*** in different tissues. Table 13. Number of ***NAC*** genes in three species.

Supplementary Material 2: Figure 1. Representative HPLC chromatograms for quantification of secondary metabolites. (A) HPLC chromatogram of 10-DAB. (B) HPLC chromatogram of paclitaxel.

Supplementary Material 3: Figure 2. Sequence alignment of TyuNAC domains in amino acid sequences. Subdomains (A-D) are shown by lines.

Supplementary Material 4: Figure 3. Analysis of cis-regulatory element of key enzyme gene promoters in secondary metabolite synthesis.

Supplementary Material 5: Figure 4. Content determination of paclitaxel and 10-DAB under MeJA treatment and up-regulation of paclitaxel biosynthesis-related genes. (A-F) Expression of paclitaxel biosynthesis-related genes in ***T. yunnanensis*** after MeJA treatment. Three biological replicates were performed for each experiment. TS, taxadiene synthase; TAT, taxadien-5a-olO-acetyltransferase; TBT, taxane 2a-O-benzoyltransferase; DBAT, 10-deacetylbaccatin-III-10-b-O-acetyltransferase; BAPT, baccatin III:3-amino-3-phenylpropanoyltransferase; DBTNBT, 30-N-debenzoyl-20-deoxytaxol-N-benzoyltransferase; Different letters in orange and blue indicate statistically significant differences ($P < 0.05$) among differentiated tissues for leaf and bark, respectively, as determined by one-way ANOVA test. (G-H) Determination of paclitaxel and 10-DAB contents under MeJA treatment by HPLC. Different lowercase letters indicate statistically significant differences among groups ($P < 0.05$) as determined by Tukey's test.

Supplementary Material 6: Figure 5. Summary figure synthesizing evolution, expression, and potential roles in paclitaxel biosynthesis of ***TyuNAC*** genes.

Acknowledgements

The author thanks the lab members for assistance. This study was carried out with the support of molecular laboratory of college of forestry, sichuan agricultural university.

Authors' contributions

JF and YW: Investigation, Conceptualization, Writing– original draft. MD and QH: Methodology, Software, Data curation. GW, SG and QL: Investigation, Methodology. MJ: Visualization, Resources. GW and XH: Writing– review &editing, Conceptualization, Supervision.

Funding

This research was funded by Sichuan Province Innovative Talent Funding Project for Postdoctoral Fellows (X H, 2322999070), Central Finance Forestry and Grassland Science and Technology Promotion Demonstration Project ([2023]9), Research Initiation Fund (X H, 031/2222996047).

Data availability

The genome sequence, protein sequences, and annotation file of T. yunnanensis and G. biloba were obtained from the 1 K Medicinal Plant Genome Database (http://www.herbgenome.com/) and Ginkgo Genome Database (https://ginkgo.zju.edu.cn/). The genome data of P. amurense, C. roseus and S. miltiorrhiza. were obtained from the Figshare (https://doi.org/10.6084/m9.figshare.27310872.v1), Dryad Digital Repository (https://doi.org/10.5061/dryad.d2547d851) and National Genomic Science Data Center (https://ngdc.cncb.ac.cn/) BioProject no.GWHDOEA00000000. The transcriptome data of 5 tissues (bark, leaf, root, stem, and twig bark) of T. yunnanensis, were retrieved from the National Center for Bioinformation database under the BioProject no. PRJNA661543.

Declarations

Ethics approval and consent to participate

The *T. yunnanensis* materials were obtained from Dujiangyan City, Sichuan Province, Professor Xiong Huang ensures that we have permission to collect and culture the *T. yunnanensis*. The plant in this study was identified as *T. yunnanensis* by Professor Xiaohong Chen, and the proof specimen of this species is stored in the Herbarium of Institute of Botany, Chinese Academy of Sciences. The deposition numbers are 02015359. The study was conducted in accordance with the relevant guidelines in Sichuan Agricultural University.

Consent for publication
Not applicable.

Competing interests
The authors declare no competing interests.

Author details
[1]Forest Ecology and Conservation in the Upper Reaches of the Yangtze River Key Laboratory of Sichuan Province, Sichuan Agricultural University, Chendu 610000, China
[2]Sichuan Mt. Emei Forest Ecosystem National Observation and Research Station, Sichuan Agricultural University, Chendu 610000, China
[3]National Forestry and Grassland Southwest Engineering Technology Research Centre of Taxus, Sichuan Agricultural University, Chengdu 610000, China

Received: 19 March 2025 / Accepted: 15 July 2025
Published online: 31 July 2025

References

1. Fan J, Huang X, Dou M, Tang S, Wang G, Fan Y, Luo A, Wang G, Wang Y. Structural characterization and immunoenhancing properties of polysaccharide CPTM-P1 from *Taxus media*. Molecules. 2024;29(6):1370.
2. Möller M, Liu J, Li Y, Li J, Ye L, Mill R, Thomas P, Li D, Gao L. Repeated intercontinental migrations and recurring hybridizations characterise the evolutionary history of yew (Taxus L.). Mol Phylogenet Evol. 2020;153:106952.
3. Song C, Fu F, Yang L, Niu Y, Tian Z, He X, Yang X, Chen J, Sun W, Wan T, Zhang H, Yang Y, Xiao T, Dossa K, Meng X, Cao F, Van de Peer Y, Wang G, Chen S. *Taxus yunnanensis* genome offers insights into gymnosperm phylogeny and taxol production. Commun Biol. 2021;4(1):1203.
4. Jia X, Feng S, Zhang H, Liu X. Plastome phylogenomics provide insight into the evolution of *Taxus*. Forests. 2022;13(10):1590.
5. Poudel RC, Gao LM, Moller M, Baral SR, Uprety Y, Liu J, Li DZ. Yews (*Taxus*) along the Hindu Kush-Himalayan region: exploring the ethnopharmacological relevance among communities of Mongol and Caucasian origins. J Ethnopharmacol. 2013;147(1):190–203.
6. Ohtsuki K, Miyai S, Yamaguchi A, Morikawa K, Okano T. Biochemical characterization of novel lignans isolated from the wood of *Taxus yunnanensis* as effective stimulators for glycogen synthase kinase-3beta and the phosphorylation of basic brain proteins by the kinase in vitro. Biol Pharm Bull. 2012;35(3):385–93.
7. Miao YC, Lang XD, Zhang ZZ, Su JR, Rennenberg H. Phylogeography and genetic effects of habitat fragmentation on endangered *Taxus yunnanensis* in southwest China as revealed by microsatellite data. Plant Biol. 2014;16(2):365–74.
8. Zhang HJ, Tadeda Y, Sun HD. Taxanes from *Taxus yunnanensis*. Phytochemistry. 1995;39(5):1147–51.
9. Yu C, Luo X, Zhan X, Hao J, Zhang L, Song YL, Shen C, Dong M. Comparative metabolomics reveals the metabolic variations between two endangered *Taxus* species (*T. fuana* and *T. yunnanensis*) in the Himalayas. BMC Plant Biol. 2018;18: 1–12.
10. Li Y, Huang S, Zhang J, Bu F, Lin T, Zhang Z, Xiong X. A protocol of homozygous haploid callus induction from endosperm of *Taxus chinensis* Rehd. var. *mairei*. SpringerPlus. 2016;5(1):659.
11. Yuan H, Guo H, Luan X, He M, Li F, Burnett J, Truchan N, Sun D. Albumin nanoparticle of paclitaxel (Abraxane) decreases while taxol increases breast cancer stem cells in treatment of triple negative breast cancer Mol. Pharm. 2020;17(7):2275–86.
12. Zheng L, Wen G, Yao Y, Li X, Gao F. Design, synthesis, and anticancer activity of natural product hybrids with paclitaxel side chain inducing apoptosis in human colon cancer cells. Nat Prod Commun. 2020;15(4): 1934578.
13. Zhang Y, Wiese L, Fang H, Alseekh S, Perez DSL, Scossa F, Molloy J, Christmann M, Fernie AR. Synthetic biology identifies the minimal gene set required for paclitaxel biosynthesis in a plant chassis. Mol Plant. 2023;16(12):1951–61.
14. Jiang B, Gao L, Wang H, Sun Y, Zhang X, Ke H, Liu S, Ma P, Liao Q, Wang Y, Wang H, Liu Y, Du R, Rogge T, Li W, Shang Y, Houk KN, Xiong X, Xie D, Huang S, Lei X, Yan J. Characterization and heterologous reconstitution of *Taxus* biosynthetic enzymes leading to baccatin III. Sci. 2024;383(6683):622–9.
15. Liu JC, De La Peña R, Tocol C, Sattely ES. Reconstitution of early paclitaxel biosynthetic network. Nat Commun. 2024;15(1):1419.
16. Zhao Y, Liang F, Xie Y, Duan Y, Andeadelli A, Pateraki I, Makris AM, Pomorski TG, Staerk D, Kampranis SC. Oxetane ring formation in taxol biosynthesis is catalyzed by a bifunctional cytochrome P450 enzyme. J Am Chem Soc. 2024;146(1):801–10.
17. Schneider F, Samarin K, Zanella S, Gaich T. Total synthesis of the complex taxane diterpene canataxpropellane. Science. 2020;367(6478):676–81.
18. Rashid A, Khajuria M, Ali V, Faiz S, Jamwal S, Vyas D. Genome-wide identification and expression profiling of WRKY family suggest their potential role in cannabinoid regulation in *Cannabis sativa* L. Ind Crop Prod. 2023;206:117706.
19. Fu C, Liu M. Genome-wide identification and molecular evolution of NAC gene family in *Dendrobium nobile*. Front Plant Sci. 2023;14: 1232804.
20. Shengmiao L, Xin D, Yue L, Lihua Y, Xiwang K, Yuhu Z. Genome-wide identification of the *NAC* family genes of adzuki bean and their roles in rust resistance through jasmonic acid signaling. BMC Genomics. 2025;26(1): 283.
21. Guo S, Dai S, Singh PK, Wang H, Wang Y, Tan J, Wee W, Ito T. A membrane-bound NAC-like transcription factor OsNTL5 represses the flowering in *Oryza sativa*. Front Plant Sci. 2018;9: 555.
22. Jin JF, Wang ZQ, He QY, Wang JY, Li PF, Xu JM, Zheng SJ, Fan W, Yang JL. Genome-wide identification and expression analysis of the NAC transcription factor family in tomato (*Solanum lycopersicum*) during aluminum stress. BMC Genomics. 2020;21(1):214–88.
23. Olsen AN, Ernst HA, Leggio LL, Skriver K. NAC transcription factors: structurally distinct, functionally diverse. Trends Plant Sci. 2005;10(2):79–87.
24. Nuruzzaman M, Sharoni AM, Kikuchi S. Roles of NAC transcription factors in the regulation of biotic and abiotic stress responses in plants. Front Microbiol. 2013;4:248.
25. Zhang L, Yao L, Zhang N, Yang J, Zhu X, Tang X, Calderon-Urrea A, Si H. Lateral root development in potato is mediated by Stu-mi164 regulation of NAC transcription factor. Front Plant Sci. 2018;9: 383.
26. Kucukoglu M. A novel NAC domain transcription factor XVP controls the balance of xylem formation and cambial cell divisions. New Phytol. 2020;226(1):5–7.
27. El MY, Akabane K, Hiratsu K, Satoh-Nagasawa N, Wabiko H. The NAC transcription factor gene *OsY37* (ONAC011) promotes leaf senescence and accelerates heading time in rice. Int J Mol Sci. 2017;18(10):2165. https://doi.org/10.3390/ijms18102165
28. Wang J, Wang Y, Zhang J, Ren Y, Li M, Tian S, Yu Y, Zuo Y, Gong G, Zhang H, Guo S, Xu Y. The NAC transcription factor ClNAC68 positively regulates sugar content and seed development in watermelon by repressing ClINV and ClGH3. 6. Hortic Res. 2021;8(1):214.
29. Li M, Chen R, Jiang Q, Sun X, Zhang H, Hu Z. *GmNAC06*, a NAC domain transcription factor enhances salt stress tolerance in soybean. Plant Mol Biol. 2021;105(3):333–45.
30. Guo W, Zhang J, Zhang N, Xin M, Peng H, Hu Z, Ni Z, Du J. The wheat NAC transcription factor TaNAC2l is regulated at the transcriptional and post-translational levels and promotes heat stress tolerance in transgenic *Arabidopsis*. PLoS One. 2015;10(8):e0135667.
31. Wang Z, Ni L, Liu D, Fu Z, Hua J, Lu Z, Liu L, Yin Y, Li H, Gu C. Genome-wide identification and characterization of NAC family in *Hibiscus hamabo* Sieb. et Zucc. under various abiotic stresses. Int J Mol Sci. 2022;23(6): 3055.
32. Yan H, Ma G, Da Teixeira Silva JA, Qiu L, Xu J, Zhou H, Wei M, Xiong J, Li M, Zhou S, Wu J, Tang X. Genome-wide identification and analysis of NAC transcription factor family in two diploid wild relatives of cultivated sweet potato uncovers potential NAC genes related to drought tolerance. Front Genet. 2021;12:744220.
33. Lv Z, Wang S, Zhang F, Chen L, Hao X, Pan Q, Fu X, Li L, Sun X, Tang K. Overexpression of a novel NAC domain-containing transcription factor gene (*AaNAC1*) enhances the content of artemisinin and increases tolerance to drought and *Botrytis cinerea* in *Artemisia annua*. Plant Cell Physiol. 2016;57(9):1961–71.
34. Kumar R, Das S, Mishra M, Choudhury DR, Sharma K, Kumari A, Singh R. Emerging roles of NAC transcription factor in medicinal plants: progress and prospects. 3 Biotech. 2021;11(10):1–14.
35. Ma W, Kang X, Liu P, She K, Zhang Y, Lin X, Li B, Chen Z. The NAC-like transcription factor CsNAC7 positively regulates the caffeine biosynthesis-related gene *yhNMT1* in *Camellia sinensis*. Hortic Res. 2022;9:uhab046.
36. Kumar R, Kumar C, Roy Choudhury D, Ranjan A, Raipuria RK, Dubey KKD, Mishra A, Kumar C, Manzoor MM, Kumar A, Kumari A, Singh K, Singh GP, Singh R. Isolation, characterization, and expression analysis of nac transcription factor from *Andrographis paniculata* (Burm. F.) Nees and their role in andrographolide production. Genes. 2024;15(4): 422.

37. Nieuwenhuizen NJ, Chen X, Wang MY, Matich AJ, Perez RL, Allan AC, Green SA, Atkinson RG. Natural variation in monoterpene synthesis in kiwifruit: transcriptional regulation of terpene synthases by NAC and ETHYLENE-INSENSITIVE3-like transcription factors. Plant Physiol. 2015;167(4):1243–58.
38. Zhu M, Chen G, Zhou S, Tu Y, Wang Y, Dong T, Hu Z. A new tomato NAC (NAM/ATAF1/2/CUC2) transcription factor, SlNAC4, functions as a positive regulator of fruit ripening and carotenoid accumulation. Plant Cell Physiol. 2014;55(1):119–35.
39. Jiang T, Zhang Y, Zuo G, Luo T, Wang H, Zhang R, Luo Z. Transcription factor PgNAC72 activates *dammarenediol synthase* expression to promote ginseng saponin biosynthesis. Plant Physiol. 2024;195(4):2952–69.
40. Zhang S, Xu T, Ren Y, Song L, Liu Z, Kang X, Li Y. The NAC transcription factor family in *Eucommia ulmoides*: genome-wide identification, characterization, and network analysis in relation to the rubber biosynthetic genes. Front Plant Sci. 2023;14:1030298.
41. Osuna L, Tapia N, Cusidó R, Palazón J, Bonfill M, Zamilpa A, López-Upton J, Cruz-Sosa F. Taxane production induced by methyl jasmonate in free and immobilized cell cultures of mexican yew (*Taxus globosa* Schltdl). Acta Physiol Plant. 2015;37(10):1–8.
42. Bonfill MU, Bentebibel SU, Moyano EU, Palazon JU, Cusido RM, Eibl RH, Pinol MT. Paclitaxel and baccatin iii production induced by methyl jasmonate in free and immobilized cells of *Taxus baccata*. Biol Plant. 2007;51(4):647–52.
43. Yamamoto S, Tabuchi F, Tanaka R, Hayashi S, Miyasaka H. Effect of methyl jasmonate on production of paclitaxel and related taxanes in a hydrophobic ionic liquid-medium two phase culture system. Solvent Extr Res Dev. 2019;26(2):105–9.
44. Kim BJ, Gibson DM, Shuler ML. Relationship of viability and apoptosis to Taxol production in *Taxus* sp. suspension cultures elicited with methyl jasmonate. Biotechnol Progr. 2005;21(3):700–7.
45. Linden JC, Phisalaphong M. Oligosaccharides potentiate methyl jasmonate-induced production of paclitaxel in *Taxus canadensis*. Plant Sci. 2000;158(1–2):41–51.
46. Yu C, Hou K, Zhang H, Liang X, Chen C, Wang Z, Wu Q, Chen G, He J, Bai E, Li X, Du T, Wang Y, Wang M, Feng S, Wang H, Shen C. Integrated mass spectrometry imaging and single-cell transcriptome atlas strategies provide novel insights into taxoid biosynthesis and transport in *Taxus mairei* stems. Plant J. 2023;115(5):1243–60.
47. Bailey TL, Boden M, Buske FA, Frith M, Grant CE, Clementi L, Ren J, Li WW, Noble WS. MEME SUITE: tools for motif discovery and searching. Nucleic Acids Res. 2009;37:W202–8.
48. Kumar S, Stecher G, Tamura K. MEGA7: molecular evolutionary genetics analysis version 7.0 for bigger datasets. Mol Biol Evol. 2016;33(7):1870–4.
49. Subramanian B, Gao S, Lercher MJ, Hu S, Chen WH. Evolview v3: a webserver for visualization, annotation, and management of phylogenetic trees. Nucleic Acids Res. 2019;47(W1):W270-5.
50. Chen C, Chen H, Zhang Y, Thomas HR, Frank MH, He Y, Xia R. Tbtools: an integrative toolkit developed for interactive analyses of big biological data. Mol Plant. 2020;13(8):1194–202.
51. Voorrips RE. Mapchart: software for the graphical presentation of linkage maps and QTLs. J Hered. 2002;93(1):77–8.
52. Wang Y, Tang H, Debarry JD, Tan X, Li J, Wang X, Lee TH, Jin H, Marler B, Guo H, Kissinger JC, Paterson AH. *Mcscanx*: a toolkit for detection and evolutionary analysis of gene synteny and collinearity. Nucleic Acids Res. 2012;40(7): e49.
53. Zhang Z, Li J, Zhao X, Wang J, Wong GK, Yu J. KaKs_Calculator: calculating Ka and Ks through model selection and model averaging. Genomics Proteomics Bioinformatics. 2006;4(4):259–63.
54. Huang X, Wang W, Gong T, Wickell D, Kuo L, Zhang X, Wen J, Kim H, Lu F, Zhao H, Chen S, Li H, Wu W, Yu C, Chen S, Fan W, Chen S, Bao X, Li L, Zhang D, Jiang L, Yan X, Liao Z, Zhou G, Guo Y, Ralph J, Sederoff RR, Wei H, Zhu P, Li F, Ming R, Li Q. The flying spider-monkey tree fern genome provides insights into fern evolution and arborescence. Nat Plants. 2022;8(5):500–12.
55. Brun˘áková K, and Košuth J. Gene expression profiling in Taxus baccata L. seedlings and cell cultures. Protocols for in vitro cultures and secondary metabolite analysis of aromatic and medicinal plants. 2009. pp.249–262.
56. Fan J, Wang P, Zheng H, Saba T, Hui W, Wang J, Wang G, Gong W. Genome-wide characterization of the MADS-box gene family and expression pattern in different tissues and stresses in *Zanthoxylum armatum*. J Plant Growth Regul. 2024;43(8):2696–714.
57. Fan J, Wang J, Liu X, Zhao C, Zhou C, Saba T, Wu J, Hui W, Gong W. Responses of antioxidant enzyme activity to different fertilizer and soil moisture conditions in relation to cold resistance in *Zanthoxylum armatum*. Hortic Sci Technol. 2022;40(3):261–72.
58. Wang Z, Wong D, Wang Y, Xu G, Ren C, Liu Y, Kuang Y, Fan P, Li S, Xin H, Liang Z. Gras-domain transcription factor PAT1 regulates jasmonic acid biosynthesis in grape cold stress response. Plant Physiol. 2021;186(3):1660–78.
59. Ouwerkerk PB, Meijer AH. Yeast one-hybrid screening for DNA-protein interactions. Curr Protoc Mol Biol Chapter. 2001;55(1):12–12.
60. Wani MC, Taylor HL, Wall ME, Coggon P, Mcphail AT. Plant antitumor agents. Vi. The isolation and structure of taxol, a novel antileukemic and antitumor agent from *Taxus brevifolia*. J Am Chem Soc. 1971;93(9):2325–7.
61. Weaver BA, Bement W. How Taxol/paclitaxel kills cancer cells. Mol Biol Cell. 2014;25(18):2677–81.
62. Walker K, Croteau R. Taxol biosynthetic genes. Phytochemistry. 2001;58(1):1–7.
63. Cheng J, Wang X, Liu X, Zhu X, Li Z, Chu H, Wang Q, Lou Q, Cai B, Yang Y, Lu X, Peng K, Liu D, Liu Y, Lu L, Liu H, Yang T, Ge Q, Shi C, Liu G, Dong Z, Xu X, Wang W, Jiang H, Ma Y. Chromosome-level genome of Himalayan yew provides insights into the origin and evolution of the paclitaxel biosynthetic pathway. Mol Plant. 2021;14(7):1199–209.
64. Xiong X, Gou J, Liao Q, Li Y, Zhou Q, Bi G, Li C, Du R, Wang X, Sun T, Guo L, Liang H, Lu P, Wu Y, Zhang Z, Ro DK, Shang Y, Huang S, Yan J. The *Taxus* genome provides insights into paclitaxel biosynthesis. Nat Plants. 2021;7(8):1026–36.
65. Wu X, Wang M, Li X, Chen Y, Liao Z, Zhang D, Wen Y, Wang S. Identification and characterization of a new species of *Taxus* - *Taxus qinlingensis* by multiple taxonomic methods. BMC Plant Biol. 2024;24(1): 658.
66. Zhan X, Liang X, Lin W, Ma R, Zang Y, Wang H, Wang L, Yang Y, Shen C. Cell type specific regulation of phenolic acid and flavonoid metabolism in *Taxus mairei* leaves. Ind Crop Prod. 2024;219:118975.
67. Zhang K, Jiang L, Wang X, Han H, Chen D, Qiu D, Yang Y. Transcriptome-wide analysis of AP2/ERF transcription factors involved in regulating Taxol biosynthesis in *Taxus*× *media* Ind. Crop Prod. 2021;171:113972.
68. Cao X, Xu L, Li L, Wan W, Jiang J. TcMYB29a, an ABA-responsive R2R3-MYB transcriptional factor, upregulates taxol biosynthesis in *Taxus chinensis*. Front Plant Sci. 2022;13:804593.
69. Li S, Zhang P, Zhang M, Fu C, Yu L. Functional analysis of a WRKY transcription factor involved in transcriptional activation of the DBAT gene in *Taxus chinensis*. Plant Biol. 2023;23(1):415.
70. Cao F, Guo C, Wang X, Wang X, Yu L, Zhang H, Zhang J. Genome-wide identification, evolution, and expression analysis of the NAC gene family in chestnut (*Castanea mollissima*). Front Genet. 2024;15: 1337578.
71. Zhang M, Hou X, Yang H, Wang J, Li Y, Liu Q, Zhang C, Wang B, Chen M. The NAC gene family in the halophyte limonium bicolor: identification, expression analysis, and regulation of abiotic stress tolerance. Plant Physiol Biochem. 2024;208: 108462.
72. Du Z, You S, Yang D, Tao Y, Zhu Y, Sun W, Chen Z, Li J. Comprehensive analysis of the NAC transcription factor gene family in *Kandelia obovata* reveals potential members related to chilling tolerance. Front Plant Sci. 2022;13:1048822.
73. Ooka H, Satoh K, Hayashizaki Y, Suzuki K, Kojima K, Takahara Y, Yamamoto K, Kikuchi S, Doi K, Nagata T, Otomo Y, Mtirakami K, Matsubara K, Osato N, Kawai J, Carninci P. Comprehensive analysis of NAC family genes in *Oryza* sativa and *Arabidopsis thaliana*. DNA Res. 2003;10(6):239–47.
74. Wang N, Zheng Y, Xin H, Fang L, Li S. Comprehensive analysis of NAC domain transcription factor gene family in *Vitis vinifera*. Plant Cell Rep. 2013;32(1):61–75.
75. Liu J, Chen T, Yuan Y, Zhou J, Zhao Y, Huang L. Bioinformatics and expression analysis of NAC transcription factor genes in *Scutellaria baicalensis*. World J Tradit Chin Med. 2018;4(2):37–42.
76. Wang Z, Zhang Z, Wang P, Qin C, He L, Kong L, Ren W, Liu X, Ma W. Genome-wide identification of the NAC transcription factors family and regulation of metabolites under salt stress in *Isatis indigotica*. Int J Biol Macromol. 2023;240:124436.
77. Xu D, Wang Z, Zhuang W, Zhang F, Xie Y, Wang T. Genome-wide identification and expression pattern analysis of BAHD acyltransferase family in *Taxus mairei*. Int J Mol Sci. 2024;25(7): 3777.
78. Moore RC, Purugganan MD. The early stages of duplicate gene evolution. PNAS. 2003;100(26):15682–7.
79. Cannon SB, Mitra A, Baumgarten A, Young ND, May G. The roles of segmental and tandem gene duplication in the evolution of large gene families in *Arabidopsis thaliana*. BMC Plant Biol. 2004;4(1):10.
80. Sriyab S, Laosirisathian N, Punyoyai C, Anuchapreeda S, Tima S, Chiampanichayakul S, Chaiyana W. Nutricosmetic effects of *Asparagus officinalis*: a potent matrix metalloproteinase-1 inhibitor. Sci Rep. 2021;11(1):8772.

81. Lynch M, Conery JS. The evolutionary fate and consequences of duplicate genes. Science. 2000;290(5494):1151–5.
82. Xu Z, Tian Y, Wang J, Ma Y, Li Q, Zhou Y, Chen S. Convergent evolution of berberine biosynthesis. Sci Adv. 2024;10(48):3596.
83. Meng L, Chen S, Li D, Huang M, Zhu S. Genome-wide characterization and evolutionary expansion of poplar NAC transcription factors and their tissue-specific expression profiles under drought. Int J Mol Sci. 2022;24(1): 253.
84. Huysmans M, Buono RA, Skorzinski N, Radio MC, De Winter F, Parizot B, Mertens J, Karimi M, Fendrych M, Nowack MK. NAC transcription factors ANAC087 and ANAC046 control distinct aspects of programmed cell death in the Arabidopsis columella and lateral root cap. Plant Cell. 2018;30(9):2197–213.
85. Yu C, Luo X, Zhang C, Xu X, Huang J, Chen Y, Feng S, Zhan X, Zhang L, Yuan H, Zheng B, Wang H, Shen C. Tissue-specific study across the stem of *Taxus media* identifies a phloem-specific TmMYB3 involved in the transcriptional regulation of paclitaxel biosynthesis. Plant J. 2020;103(1):95–110.
86. Baebler Š, Camloh M, Kovač M, Ravnikar M, Žel J. Jasmonic acid stimulates taxane production in cell suspension culture of yew (*Taxus* × *media*). Planta Med. 2002;68(5):475–6.
87. Zhang JF, Gong S, Guo ZG. Effects of different elicitors on 10-deacetylbaccatin III-10-O-acetyltransferase activity and cytochrome P450 monooxygenase content in suspension cultures of *Taxus cuspidata* cells. Cell Biol Int Rep. 2010;18(1):7–13.
88. Qiao F, Cong H, Jiang X, Wang R, Yin J, Qian D, Wang Z, Nick P. De novo characterization of a *Cephalotaxus hainanensis* transcriptome and genes related to paclitaxel biosynthesis. PLoS One. 2014;9(9):e106900.
89. Sykłowska-Baranek K, Sygitowicz G, Maciejak-Jastrzębska A, Pietrosiuk A, Szakiel A. Application of priming strategy for enhanced paclitaxel biosynthesis in *Taxus*× *media* hairy root cultures. Cells. 2022;11(13):2062.
90. Li C, Zhang J, Zhang Q, Dong A, Wu Q, Zhu X, Zhu X. Genome-wide identification and analysis of the NAC transcription factor gene family in garden asparagus (*Asparagus officinalis*). Genes. 2022;13(6):976.
91. Zhang M, Chen Y, Nie L, Jin X, Liao W, Zhao S, Fu C, Yu L. Transcriptome-wide identification and screening of WRKY factors involved in the regulation of taxol biosynthesis in *Taxus chinensis*. Sci Rep. 2018;8(1): 5197.
92. Cui Y, Mao R, Chen J, Guo Z. Regulation mechanism of MYC family transcription factors in jasmonic acid signalling pathway on taxol biosynthesis. Int J Mol Sci. 2019;20(8):1843.
93. Zheng H, Fu X, Shao J, Tang Y, Yu M, Li L, Huang L, Tang K. Transcriptional regulatory network of high-value active ingredients in medicinal plants. Trends Plant Sci. 2023;28(7):856.

Publisher's Note